Charge and dielectric effects of biomolecules on electrical characteristics of nanowire FET biosensors

Jae-Hyuk Ahn, Sung-Jin Choi, Maesoon Im, Sungho Kim, Chang-Hoon Kim, Jee-Yeon Kim, Tae Jung Park, Sang Yup Lee, and Yang-Kyu Choi

Citation: Appl. Phys. Lett. **111**, 113701 (2017);
View online: https://doi.org/10.1063/1.5003106
View Table of Contents: http://aip.scitation.org/toc/apl/111/11
Published by the American Institute of Physics

Charge and dielectric effects of biomolecules on electrical characteristics of nanowire FET biosensors

Jae-Hyuk Ahn,[1] Sung-Jin Choi,[2] Maesoon Im,[3,4,5] Sungho Kim,[6] Chang-Hoon Kim,[7] Jee-Yeon Kim,[7] Tae Jung Park,[8] Sang Yup Lee,[9] and Yang-Kyu Choi[7,a)]
[1]*Department of Electronic Engineering, Kwangwoon University, Seoul 01897, Korea*
[2]*School of Electrical Engineering, Kookmin University, 77 Jeongneung-ro, Seongbuk-gu, Seoul 02707, South Korea*
[3]*Department of Ophthalmology, Henry Ford Health System, 1 Ford Place, Detroit, Michigan 48202, USA*
[4]*Department of Anatomy and Cell Biology, Wayne State University School of Medicine, 540 East Canfield Street, Detroit, Michigan 48201, USA*
[5]*Department of Electrical and Computer Engineering, Wayne State University College of Engineering, 5050 Anthony Wayne Drive, Detroit, Michigan 48202, USA*
[6]*Department of Electrical Engineering, Sejong University, Seoul 05006, South Korea*
[7]*School of Electrical Engineering, KAIST, 291 Daehak-ro, Daejeon 34141, South Korea*
[8]*Department of Chemistry, Chung-Ang University, 84 Heukseok-ro, Dongjak-gu, Seoul 06974, South Korea*
[9]*Department of Chemical & Biomolecular Engineering (BK21 Plus Program), BioProcess Engineering Research Center, Center for Systems & Synthetic Biotechnology, Institute for the BioCentury, and Bioinformatics Research Center, KAIST, 291 Daehak-ro, Daejeon 34141, Korea*

(Received 14 February 2017; accepted 25 August 2017; published online 13 September 2017)

The sensing mechanism of nanowire field effect transistor (NWFET) biosensors is investigated by taking into consideration both the charge and dielectric effects of biomolecules. The dielectric effect of the biomolecules is dominantly reflected in the linear regime, whereas the charge property is manifested in the subthreshold regime. The findings are supported by bio-experiments and numerical simulations. This study provides a rudimentary means of understanding interactions between biomolecules and NWFET biosensors. *Published by AIP Publishing.*
[http://dx.doi.org/10.1063/1.5003106]

Nanowire field effect transistors (NWFETs) have shown great feasibility for use as biosensors by virtue of their high sensitivity, low-cost, and the provision of label-free electrical detection at very low concentrations.[1–4] Intrinsic charges of the biomolecules bound on the NW surface interact electrostatically with carriers in the NW and lead to a conductance change. These electric field effects arising from the charged biomolecules have been extensively analyzed in previous studies. Many representative experimental results related to sensor response have been theoretically analyzed in terms of concentration- and time-dependences.[4–6] In addition, optimal operation conditions to detect the charges of the biomolecules have been suggested for comprehensive design considerations.[7–9] A new type of detection based on the dielectric properties of biomolecules has been reported to potentially detect neutral or weakly charged biomolecules.[10,11] When the biomolecules are filled into a nanogap (or nanocavity) between the gate and the channel, the gate capacitance in a dry environment is increased with the dielectric constant, and thus, the device conductance is modulated. To enhance this dielectric effect in biomolecule sensing, various sensor structures have been suggested and characterized with simulation and modeling.[12–14] The dielectric effect on the screening of intrinsic molecular charges has been analyzed in the presence of an aqueous solution.[15,16] Although the previous works can explain how each of the charge and dielectric properties of biomolecules affects the sensor operation, the influence of the both effects on the electrical characteristics of NWFET biosensors has not been fully understood with experimental data.[13,17] Moreover, the operation condition to maximize the charge and dielectric effects is needed to be investigated for highly sensitive detection of biomolecules. In this work, we propose a sensing mechanism, taking into consideration both the charge and dielectric properties of biomolecules, which simultaneously affect the detection of biomolecules. Through designed bio-experiments, charge and dielectric behaviors of biomolecules are observed, and the experimental findings are supported by numerical simulations. We find that the dielectric effect of the biomolecules is dominantly enhanced in the linear regime, whereas the charge effect is maximized in the subthreshold regime.

When analyzing the effects of biomolecules in NWFET biosensors, an analogy between a conventional metal-oxide-semiconductor field effect transistor (MOSFET) and the NWFET biosensor may be noted, as illustrated in Fig. 1(a). In both cases, an electrical field from a gate modulates the drain current (I_D), which flows horizontally from the drain to the source. In operation of MOSFETs, trapped charges in a gate dielectric induce the shift of a threshold voltage (V_T) near the subthreshold regime, which can be exploited in memory applications.[18] In a similar manner, a V_T shift occurs in the NWFET biosensors due to the intrinsic charges of the biomolecules bound on the NW surface, resulting in a conductance change in the NW. The electrical characteristics of the MOSFETs are mostly governed by the gate field, which is applied across the gate dielectric. For example, the vertical

a)Author to whom correspondence should be addressed: ykchoi@ee.kaist.ac.kr

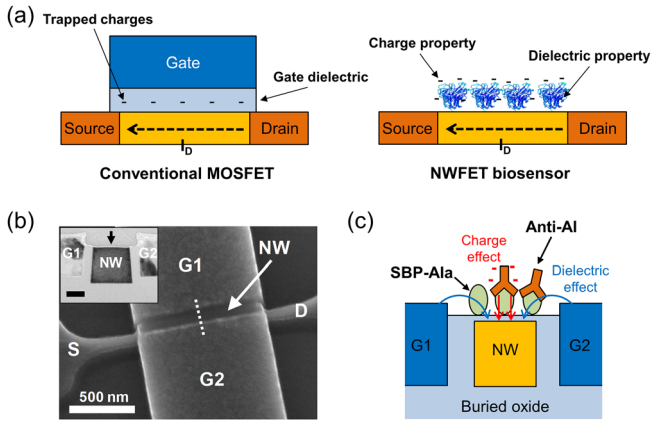

FIG. 1. (a) Schematics of a conventional MOSFET and a typical NWFET biosensor. (b) SEM image of the NWFET in the sensing region. (Inset) TEM image showing a cross-sectional view of the NWFET (scale bar = 50 nm) along the dashed line in (b). The black arrow represents the top surface of the NW, which is opened so as to immobilize biomolecules. (c) A schematic showing a NWFET in the cross-section and biomolecules interacting on the NW. The antibody of the avian influenza (anti-AI) specifically binds to SBP-AIa, which is a fusion protein including a silica binding protein (SBP) and an antigen of AI (AIa).

field is strengthened as the dielectric constant (k) of the gate dielectric increases. Hence, the on-state I_D in the linear regime is increased by the employment of a "high-k" gate dielectric material.[19] Similarly, when biomolecules are introduced onto NWFETs, k is increased ($k > 1$) from unity, corresponding to the air. Thus, it is evident that the dielectric properties from the biomolecules affect the electrical characteristics of the biosensors, especially the on-state I_D in the linear regime.

To verify the aforementioned effects of electric and dielectric properties, NWFETs were fabricated by use of a silicon-on-insulator (SOI) wafer with the aid of a top-down approach, previously reported by our group.[3,20] Figure 1(b) shows the SEM and TEM images of the fabricated NWFET. Both sidewalls of the NW are covered by gate1 (G1) and gate2 (G2), which modulate the NW conductance. A cross-sectional TEM image [inset of Fig. 1(b)] shows that the fabricated NWs have a width of 110 nm and a height of 100 nm. The thickness of the gate oxide is 30 nm. As marked with a black arrow in the inset of Fig. 1(b), the top surface of the NW is open for immobilization of biomolecules as depicted in Fig. 1(c). G1 and G2 are electrically tied, and the same gate voltage (V_G) is applied with respect to the grounded source.

To investigate the sensing mechanism taking into consideration both charge and dielectric effects, the surface antigen of the avian influenza (AI) virus and its specific antibody were used as test biomolecules, as shown in Fig. 1(c). The surface antigen of AI (AIa) was fused with a silica binding protein (SBP), which is designed to be selectively immobilized on the silica surface. Thus, SBP-AIa, a protein fused with SBP and AIa, can preferentially be immobilized onto the silicon NW surface without extra surface treatment. Details of the SBP design and immobilization procedure can be found in previous reports.[3,11] The devices were incubated at room temperature for 1 h in a SBP-AIa solution of 25 μg/ml incorporated into PBS buffer (pH 7.4). They were then washed in deionized water and dried under a flow of N_2 gas prior to the electrical measurement. SBP-AIa-functionalized devices were then incubated for 1 h in a 20 μg/ml solution containing the antibody (anti-AI) in PBS buffer, followed by the same washing and drying procedure. Anti-AI specifically bound to SBP-AIa, which was already immobilized on the NW surface. All electrical measurements were performed in a dry environment with a semiconductor parameter analyzer (HP 4156) unless otherwise mentioned.

Figure 2(a) shows the electrical characteristics of SBP-AIa-functional NWFETs before (filled square) and after (hollow square) subsequent binding of anti-AI. As shown in the log scale graph, the threshold voltage is shifted to the positive side and I_D in the subthreshold regime ($V_G = \sim -1$ V) is reduced. This is caused by negatively charged anti-AI.[3] As shown in the linear scale graph, however, I_D after anti-AI binding crosses over I_D before anti-AI binding when V_G is above -0.15 V. As outlined below, it was verified that the increment of I_D in the linear regime ($V_G = \sim -0.5$ V) is caused by the dielectric property of the biomolecules. As shown in Fig. 2(b), the maximum transconductance of the device increased after anti-AI binding. This directly shows that the k of the device is increased due to specific binding of the anti-AI; the amount of the maximum transconductance is accordingly proportional to k.[18] We observed that the increment of the maximum transconductance is also shown in the p-channel NWFETs after anti-AI binding (Fig. S1, supplementary material). In the case of n-channel NWFETs, as illustrated in Fig. 1(c), the dielectric effect stemming from the fringing field via the biomolecules is competing with the charge effect via the vertical field, as they are oppositely acting on I_D. In contrast, they unilaterally influence I_D in the case of p-channel NWFETs, and thus, a cross-over of I_D is not observed (Fig. S1, supplementary material).

As shown in Fig. 2(c), the relative change in the conductance ($\Delta G/G_0$) has a negative value in the subthreshold regime, whereas it has a positive value in the linear regime. This result shows that the charge property dominates in the subthreshold regime,[7] whereas the dielectric property is dominant in the linear regime. I_D in the linear regime is also sensitive to the source/drain contact resistance. To avoid the unwanted change in the contact resistance at each measurement, we carried out the same experiment in real-time in a wet environment, i.e., the NWFET is not surrounded by air (dry environment) but submerged in a solution medium (see Fig. S2 in the supplementary material for the I_D versus V_G curves measured in a PBS solution after SBP-AIa immobilization). The trend shown in Fig. 2(c) is consistently reproduced. The direction of $\Delta G/G_0$ is opposite in different operational regimes [Fig. 2(d)]. Specifically, $\Delta G/G_0$ upon injection of the anti-AI solution decreases in the subthreshold regime ($V_G = -1.5$ V), whereas it increases in the linear regime ($V_G = -1.0$ V). The analysis of the charge and dielectric effects of biomolecules on the biosensor operation is complicated in the presence of an aqueous solution containing water and ions. Various factors such as ionic strength, orientation of biomolecules, and electric field should be considered for the signal generation.[21] Jayant *et al.*[15] extended the previous study by Liu and Dutton[16] and highlighted the role of permittivity affecting the screening of intrinsic

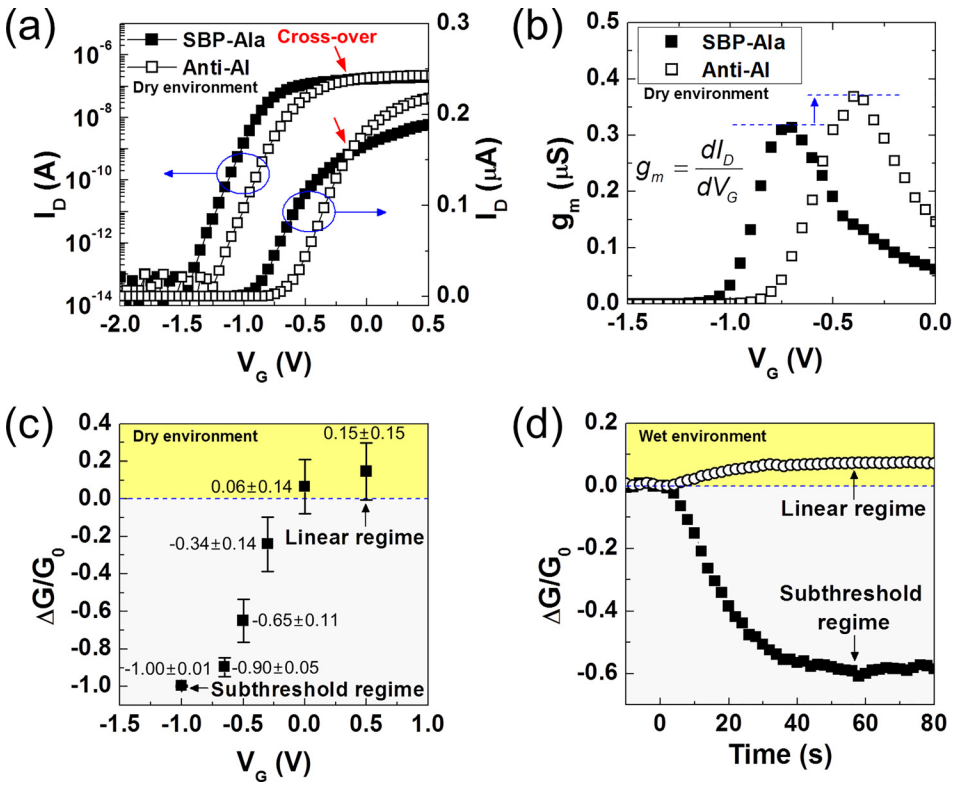

FIG. 2. (a) I_D versus V_G curves acquired in a dry environment before (filled square) and after (hollow square) binding of anti-AI to SBP-AIa at a drain voltage (V_D) of 50 mV. (b) Transconductance (g_m) as a function of V_G. (c) Relative change in conductance ($\Delta G/G_0$) as a function of the gate voltage. For this plot, anti-AI sensing data were obtained from three different devices. (d) Real-time conductance data ($\Delta G/G_0$) of the SBP-AIa-functionalized device to an anti-AI solution (20 μg/mL) at $V_G = -1.5$ V (subthreshold regime) and −1.0 V (linear regime). Introduction of the anti-AI solution occurs at time = 0 s in all experiments.

molecular charges. The permittivity difference between the molecular layer and electrolyte generates the energy barriers that ions encounter. This partition effect stems from the Born charge-dielectric interaction where an energy cost is incurred when ions diffuse from the electrolyte with a high permittivity into the molecular layer with a low permittivity. This energy penalty leads to ion exclusion within the molecular layer and in turn lower screening. In addition to the conformational flexibility of the probe biomolecule (SBP-AIa),[22] this lowered screening effect would be a possible reason why the charge of the anti-AI can be detected even in a high ionic strength electrolyte such as a 1× PBS solution (Debye length, ∼0.76 nm) [Fig. 2(d)]. However, the aforementioned theory based on the Debye length modulation could not fully explain our observation that the drain current was increased upon addition of an anti-AI solution when the NWFET is biased in the linear regime [Fig. 2(d)]. A plausible explanation is that the capacitance of the molecular layer is increased in certain conditions,[23–25] and this effect is seen as the current increment in the linear regime. The debating influence of the molecular layer on capacitance in watery environment demands further investigation in depth.

The effects of the both charge and dielectric properties on the NW conduction in a dry environment were also verified by the use of a three-dimensional device simulator (ATLAS in SILVACO Inc.[26]). As shown in the cross-sectional view depicted in Fig. 3(a), the biomolecules on the NW surface are simply modeled with a combination of the charge and dielectric layer. In this model, the sum of the thicknesses of the charge layer (t_C) and dielectric layer (t_D) is equal to the length of the target biomolecule (i.e., anti-AI), which is ∼14 nm with the vertical orientation (or fully extended configuration).[27] The charge layer to mimic a negative net charge of the biomolecule is designated as a floating with a thickness of 2 nm (see supplementary material for how to set the charge layer in the simulation). Thus, for the remaining part of the biomolecule, the thickness of the dielectric layer is set as 12 nm. The effect of t_C and t_D on the sensor response is described in the supplementary material. When the charge effect is considered solely, the dielectric constant (k) of the dielectric layer is assigned as unity ($k = 1$). It is noted that some biomolecules including biotin (pI = 3.5), streptavidin (pI = 5–6), and antibody (pI = 6.01) are negatively charged, as their pI values are lower than pH of buffer solution (pH = 7.4) (see supplementary material for the pI value of the antibody).[28] In the case of neutral or weakly charged biomolecules, the dielectric property of the biomolecules dominates the charge effect. A value of the dielectric constant in the simulation is assigned as $k = 2.0$–5.0 with consideration of the dielectric constant of biomolecules including biotin ($k = 2.6$), streptavidin ($k = 2.1$), and proteins including the antibody ($k = 4$–6).[14] As shown in Fig. 3(b), I_D is decreased and shifted to positive voltage in parallel after negative charge is introduced to the charge layer. This is because negative charge repulses the electrons from the NW surface and lowers the electron concentration.[2,29] In contrast, I_D is increased with an increased slope (dI_D/dV_G) as the dielectric constant is increased [Fig. 3(c)]. A cross-over consistent with the experimental result [Fig. 2(a)] cannot be reproduced in the both simulation conditions. Instead, the cross-over of I_D is found when the charge and dielectric parameters are combined as shown in Fig. 3(d). This result supports the fact that the both charge and dielectric effects should be considered to understand the operation of NWFET biosensors. Although the simple model of biomolecules with a combination of the charge and dielectric layer can explain the behavior of NWFET biosensors in a dry environment qualitatively, further work is required to develop a more elaborate model of

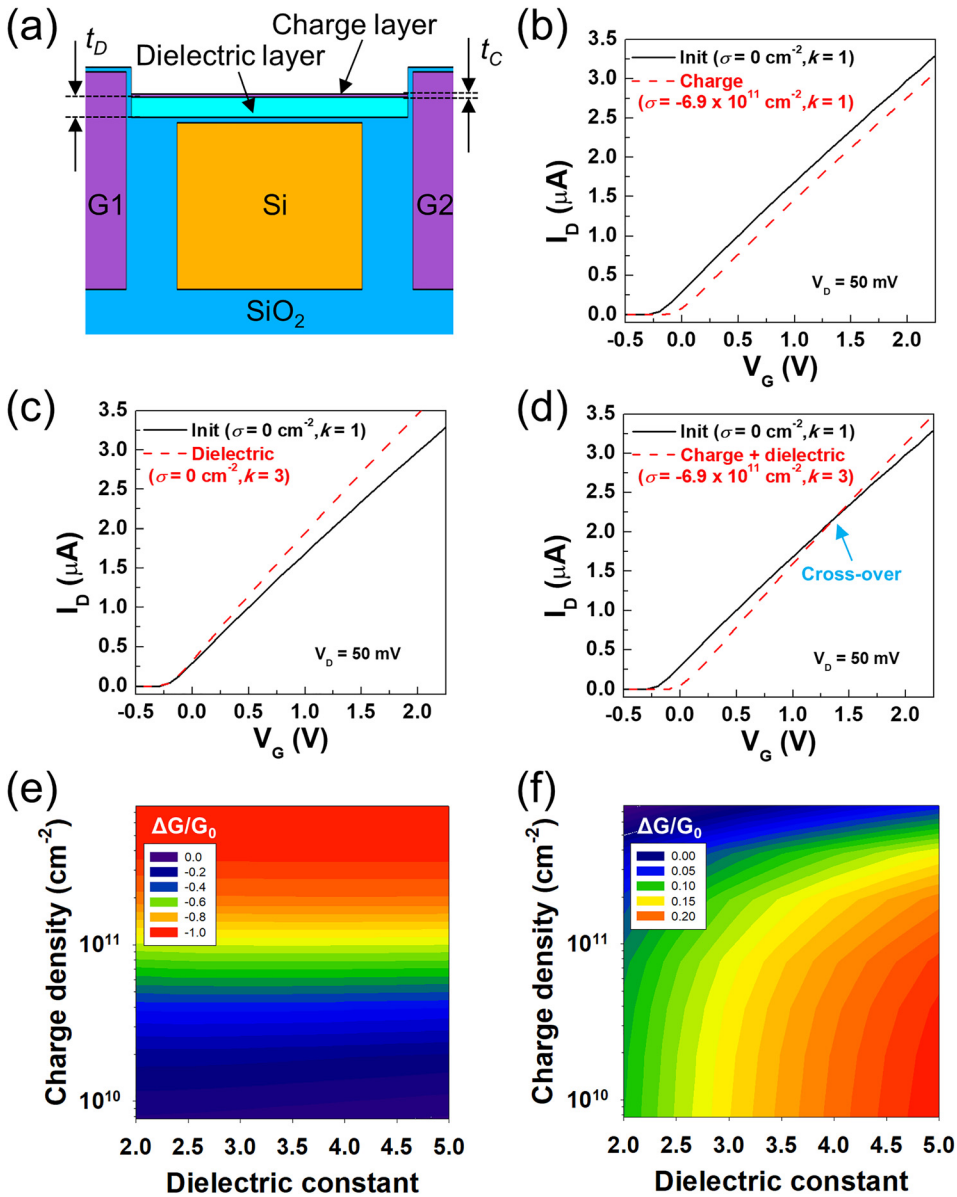

FIG. 3. (a) The device architecture used for the simulation. The figure shows a cross-section of the three-dimensional device along the direction perpendicular to the source and drain. Biomolecules bound on the top of the silicon NW are modeled as a combination of the dielectric and charge layer, where the dielectric constant (k) and the charge density (σ) are set. Thicknesses of the dielectric layer (t_D) and charge layer (t_C) are 12 and 2 nm, respectively. (b) I_D versus V_G from the simulated data before (black) and after (red) the employment of negative charge density. The value of charge density ($\sigma = -6.9 \times 10^{11}\,\mathrm{cm}^{-2}$), which is extracted from the measured V_T shift of 0.2 V after the anti-AI binding as shown in Fig. 2(a), is used as a reference. This charge density corresponds to approximately 10% coverage of the anti-AI molecules on the surface (see supplementary material). (c) I_D versus V_G from the simulated data before (black) and after (red) setting the dielectric constant of 3. (d) I_D versus V_G from the simulated data before (black) and after (red) setting both the negative charge density ($\sigma = -6.9 \times 10^{11}\,\mathrm{cm}^{-2}$) and the dielectric constant of 3. (e) and (f) Simulation results with consideration of the charge and dielectric effects of biomolecules. The relative change in conductance ($\Delta G/G_0$) as a function of the charge density and the dielectric constant at (e) $V_G = -0.3$ V (subthreshold regime) and (f) $V_G = 1.5$ V (linear regime) is also shown.

biomolecules and to provide physical quantities of biomolecules by fitting experimental data with simulation data.

Figure 3(e) shows the normalized conductance data ($\Delta G/G_0$) in the subthreshold regime as a function of the charge density and dielectric constant. The response increases as the charge density increases, whereas the response is not significantly affected by the dielectric constant. Figure 3(f) exhibits the same normalized conductance data in the linear regime. The results show that the response increases as the dielectric constant increases. However, the response according to the charge density does not vary substantially. It is thus inferred that the charge property governs in the subthreshold regime, while the dielectric property dominates in the linear regime. This result is also shown in the simulated I_D versus V_G curves in both log and linear scales for different dielectric constant and charge density (Fig. S5, supplementary material).

One of the key parameters in biosensors is the signal-to-noise ratio (SNR), which is defined as the ratio of signal power to the noise power. It is reported that the minimum input-referred noise is achieved when the FET is biased in the subthreshold regime.[30] When the charge of biomolecules is considered, a peak value of SNR is achieved in subthreshold operation.[7,30] However, when the charge of biomolecules is assumed to be neutral and the dielectric constant is considered, it is observed that the input signal power is much lowered in the subthreshold regime (Fig. S6, supplementary material). Thus, the SNR in the subthreshold regime can be degraded, while the SNR in the linear regime is expected to be improved. It means that SNR is a function of not only the bias condition but also the property of biomolecules.

In summary, we presented a comprehensive sensing mechanism of nanowire FET based biosensors by taking into consideration the both charge and dielectric properties arising from biomolecules. Taking inspiration from the effect of the gate dielectric in conventional MOSFETs, the dielectric behavior of the biomolecule was experimentally observed in n-channel nanowires. Unlike the charge effect, the dielectric effect of the biomolecules dominated in the linear regime. Thus, the sensing regime for achieving a maximum response can be tunable according to the dependence on the property of the biomolecules. This study will help researchers analyze the sensor response by considering both the charge and

dielectric effects of biomolecules and attain a better understanding of the overall behaviors of nanowire FET based biosensors.

See supplementary material for a typical biosensing experiment with p-channel nanowire FETs, setting of the charge layer in the simulation, I_D versus V_G curves measured in a PBS solution after SBP-AIa immobilization, calculation of the charge of an anti-AI, the effect of the thicknesses of the dielectric layer and charge layer, simulated I_D versus V_G curves for different dielectric constants and charge densities, and input signal power for calculating the signal-to-noise ratio.

This research was supported by Grant No. 08K1401-00210 from the Center for Nanoscale Mechatronics & Manufacturing, one of the 21st Century Frontier Research Programs supported by the Korea Ministry of Education, Science and Technology (MEST). It was also supported by the National Research and Development Program (Grant No. 2010-0002108) for the development of biomedical function monitoring biosensors and the National Research Foundation of Korea funded by the Korean government (Grant No. 2010-0018931). This work was supported by the National Research Foundation of Korea (NRF) Grant funded by the Korea government (MSIP; Ministry of Science, ICT and Future Planning) (No. 2017R1C1B5017451). The present research has been partially conducted by the Research Grant of Kwangwoon University in 2016. The work of SYL was supported by the Intelligent Synthetic Biology Center through the Global Frontier Project (2011-0031963) of the Ministry of Science and ICT.

[1]Y. Cui, Q. Wei, H. Park, and C. M. Lieber, Science **293**, 1289 (2001).
[2]G. Zheng, F. Patolsky, Y. Cui, W. U. Wang, and C. M. Lieber, Nat. Biotechnol. **23**, 1294 (2005).
[3]J.-H. Ahn, S.-J. Choi, J.-W. Han, T. J. Park, S. Y. Lee, and Y.-K. Choi, Nano Lett. **10**, 2934 (2010).
[4]X. Duan, Y. Li, N. K. Rajan, D. A. Routenberg, Y. Modis, and M. A. Reed, Nat. Nanotechnol. **7**, 401 (2012).
[5]P. R. Nair and M. A. Alam, IEEE Trans. Electron Devices **54**, 3400 (2007).
[6]P. R. Nair and M. A. Alam, Nano Lett. **8**, 1281 (2008).
[7]X. P. A. Gao, G. Zheng, and C. M. Lieber, Nano Lett. **10**, 547 (2010).
[8]E. Stern, R. Wagner, F. J. Sigworth, R. Breaker, T. M. Fahmy, and M. A. Reed, Nano Lett. **7**, 3405 (2007).
[9]R. Elnathan, M. Kwiat, A. Pevzner, Y. Engel, L. Burstein, A. Khatchtourints, A. Lichtenstein, R. Kantaev, and F. Patolsky, Nano Lett. **12**, 5245 (2012).
[10]H. Im, X.-J. Huang, B. Gu, and Y.-K. Choi, Nat. Nanotechnol. **2**, 430 (2007).
[11]B. Gu, T. J. Park, J.-H. Ahn, X.-J. Huang, S. Y. Lee, and Y.-K. Choi, Small **5**, 2407 (2009).
[12]J.-M. Choi, J.-W. Han, S.-J. Choi, and Y.-K. Choi, IEEE Trans. Electron Devices **57**, 3477 (2010).
[13]R. Narang, K. V. S. Reddy, M. Saxena, R. S. Gupta, and M. Gupta, IEEE Trans. Electron Devices **59**, 2809 (2012).
[14]Ajay, R. Narang, M. Saxena, and M. Gupta, IEEE Trans. Electron Devices **62**, 2636 (2015).
[15]K. Jayant, K. Auluck, M. Funke, S. Anwar, J. B. Phelps, P. H. Gordon, S. R. Rajwade, and E. C. Kan, Phys. Rev. E **88**, 012802 (2013).
[16]Y. Liu and R. W. Dutton, J. Appl. Phys. **106**, 014701 (2009).
[17]C.-H. Kim, C. Jung, K.-B. Lee, H. G. Park, and Y.-K. Choi, Nanotechnology **22**, 135502 (2011).
[18]S. M. Sze, *Physics of Semiconductor Devices*, 2nd ed. (Wiley, New York, 1981).
[19]G. D. Wilk, R. M. Wallace, and J. M. Anthony, J. Appl. Phys. **89**, 5243 (2001).
[20]J.-H. Ahn, J.-Y. Kim, M.-L. Seol, D. J. Baek, Z. Guo, C.-H. Kim, S.-J. Choi, and Y.-K. Choi, Appl. Phys. Lett. **102**, 083701 (2013).
[21]K. Jayant, K. Auluck, S. Rodriguez, Y. Cao, and E. C. Kan, Phys. Rev. E **89**, 052817 (2014).
[22]J.-H. Ahn, J.-Y. Kim, K. Choi, D.-I. Moon, C.-H. Kim, M.-L. Seol, T. J. Park, S. Y. Lee, and Y.-K. Choi, IEEE Trans. Electron Devices **59**, 2243 (2012).
[23]C. Saby, N. Jaffrezic-Renault, C. Martelet, B. Colin, M. H. Charles, T. Delair, and B. Mandrand, Sens. Actuators, B **16**, 458 (1993).
[24]A. B. Kharitonov, J. Wasserman, E. Katz, and I. Willner, J. Phys. Chem. B **105**, 4205 (2001).
[25]S. Ingebrandt, Y. Han, F. Nakamura, A. Poghossian, M. J. Schöning, and A. Offenhäusser, Biosens. Bioelectron. **22**, 2834 (2007).
[26]Silvaco Int., *ATLAS User's Manual* (Santa Clara, California, 2009).
[27]A. Kim, C. S. Ah, C. W. Park, J.-H. Yang, T. Kim, C.-G. Ahn, S. H. Park, and G. Y. Sung, Biosens. Bioelectron. **25**, 1767 (2010).
[28]S. Kim, D. Baek, J.-Y. Kim, S.-J. Choi, M.-L. Seol, and Y.-K. Choi, Appl. Phys. Lett. **101**, 073703 (2012).
[29]A. Kim, C. S. Ah, H. Y. Yu, J.-H. Yang, I.-B. Baek, C.-G. Ahn, C. W. Park, and M. S. Jun, Appl. Phys. Lett. **91**, 103901 (2007).
[30]M. J. Deen, M. W. Shinwari, J. C. Ranuárez, and D. Landheer, J. Appl. Phys. **100**, 074703 (2006).